Journal of the Korean Astronomical Society
54: 9 ∼ 16, 2021 February
https://doi.org/10.5303/JKAS.2021.54.1.9
pISSN: 1225-4614 · eISSN: 2288-890X
http://jkas.kas.org

Conceptual Structural Design and Comparative Power System Analysis of Ozone Dynamics Investigation Nano-satellite (ODIN)

Nuri Park[1], Euidong Hwang[1], Yeonju Kim[1], Yeongju Park[1], Deokhun Kang[2], Jonghoon Kim[2], Ik-seon Hong[1], Gyeongbok Jo[1], Hosub Song[1,3], Kyoung Wook Min[4], and Yu Yi[1]

[1]Department of Astronomy and Space Science, Chungnam National University, Daejeon 34314, Republic of Korea; nuripark2011@gmail.com, euyiyu@cnu.ac.k
[2]Department of Electrical Engineering, Chungnam National University, Daejeon 34314, Republic of Korea
[3]Korea Astronomy and Space Science Institute, Daejeon 34055, Republic of Korea
[4]Department of Physics, Korea Advanced Institute of Science and Technology, 34141, Daejeon, Republic of Korea

Received April 23, 2020; accepted January 5, 2021

Abstract: The Ozone Dynamics Investigation Nano-Satellite (ODIN) is a CubeSat design proposed by Chungnam National University as contribution to the CubeSat Competition 2019 sponsored by the Korean Aerospace Research Institute (KARI). The main objectives of ODIN are (1) to observe the polar ozone column density (latitude range of 60° to 80° in both hemispheres) and (2) to investigate the chemical dynamics between stratospheric ozone and ozone depleting substances (ODSs) through spectroscopy of the terrestrial atmosphere. For the operation of ODIN, a highly efficient power system designed for the specific orbit is required. We present the conceptual structural design of ODIN and an analysis of power generation in a sun synchronous orbit (SSO) using two different configurations of 3U solar panels (a deployed model and a non-deployed model). The deployed solar panel model generates 189.7 W through one day which consists of 14 orbit cycles, while the non-deployed solar panel model generates 152.6 W. Both models generate enough power for ODIN and the calculation suggests that the deployed solar panel model can generate slightly more power than the non-deployed solar panel model in a single orbit cycle. We eventually selected the non-deployed solar panel model for our design because of its robustness against vibration during the launch sequence and the capability of stable power generation through a whole day cycle.

Key words: space vehicles — instrumentation: spectrographs

1. Introduction

A CubeSat is a small satellite classified as a nano-satellite (satellites that are not heavier than 10 kg). The size of CubeSats is commonly expressed in units of U where 1U indicates a 10 cm cube. Because of their low cost and relatively short time span required for development, the number of launched CubeSats has increased exponentially since 2005 (Villela et al. 2019). Originally, CubeSats served mainly as training tools for satellite development. Nowadays, CubeSats are developed for testing technologies and science mission concepts (Desselle et al. 2017; Iuzzolino et al. 2017). Recently, CubeSats have been studied for various scientific missions on lunar orbits (Song et al. 2019; Lee et al. 2017).

Since 2012, the Korean Aerospace Research Institute (KARI) has hosted CubeSat design contests for universities and industrial companies to promote domestic technological advancement in CubeSat building (Han et al. 2017). Project ODIN is one of the six selected participants in the '2019 CubeSat Contest – Science Mission Part'. The main objective of the project is to design a 3U (10 cm × 10 cm × 30cm) CubeSat to retrieve spectroscopic data of the terrestrial atmosphere. Using the retrieved data we expect to be able to calibrate the ozone and trace gas (activated ozone depleting substances [ODSs]) column density of both polar regions (latitudes 60°–80°) to enhance our understanding of the atmospheric chemical dynamics in the stratosphere.

The ozone layer is the part of the terrestrial atmosphere where the number density of ozone molecules is the highest. It is located in the stratosphere (altitudes 20–50 km) and prevents the penetration of UV-B radiation which is harmful to many life forms. The importance of monitoring the ozone column density and ODSs has been evident since the first observations of seasonal extreme depletion of Antarctic stratospheric ozone, today known as the ozone hole (Farman et al. 1985). Follow-up studies suggest that the Montreal Protocol, an international agreement aimed at the protection of stratospheric ozone established in 1989, was helpful for the recovery of the ozone layer (Weatherhead & Andersen 2006). However, some observations indicate an Arctic stratospheric ozone loss (Manney et al. 2011). In addition, there is evidence for an increasing abundance of the main ingredients of ODSs nearby China (Rigby et al. 2019).

The scientific mission of ODIN is focused on the detection of variations of the ozone column density above both polar regions through ultraviolet-to-visible (UV-VIS, 200–700 nm) spectroscopy. We aim at monitoring the ozone density and ODSs density variations from October through March covering a full cycle of the

Corresponding author: Yu Yi

Table 1
Overall requirements of ODIN

Category	Requirements
Orbit	700 km
Mass	Max 4 kg
Mission Lifetime	6 months
Control Method	3-axis
Bus Voltage	3.3 V, 5 V
Bus Communication	CAN/I2C/UART
Data Communication	UART/I2C
Control Frequency	UHF
Data Transmission Frequency	S-band

Table 2
Compartments used in conceptual structural design

Subsystem	Item	Model
CDHS	OBC	DSW OBC
ADCS	Sun Sensor	nanoSSOC-D60
	GPS	OEM719
	Reaction Wheel	CubeWheel
	Magnetorquer Board	DSW MTQR
Interface	Interface Board	DSW Board
EPS	EPS board	nanopower p60
	Battery	nanopower bp4
	Solar Panel	Solar Panel 1U
	Solar Panel	Solar Panel 3U
COMM	UHF Transceiver	AX100
	UHF Antenna	ANT430
	S-Band Transmitter	CPUT Trans
	S-Band Antenna	CPUT Pacth Ant
STS	Structure	3U CubeSat Struc.
Payloads	Optical Cam	C3D
	Spectrometer	HDV UV-VIS

Antarctic ozone column density which is distinctively low in October and is fully restored by March. The requirements for ODIN to successfully accomplish its scientific missions are presented in Table 1. The design lifetime of ODIN is one year, to monitor annual ozone variations and annual flows of ODSs. Since we focus on understanding the annual variations of ozone density, chemical dynamics, and movement of ODSs, the required minimum lifetime of ODIN is 6 months. Successful completion of the ODIN mission will provide invaluable information for understanding the current status of polar stratospheric ozone.

In this study, we present the conceptual structural design and comparative power system analysis of ODIN. Since the structure of a CubeSat is restricted by the frames of the cube elements and the mass of a CubeSat is limited to 4 kg, an efficient arrangement of all functional compartments is crucial. We arranged all the required compartments inside the 3U CubeSat frame, in compliance with the structural (volume) and mass constraints.

Failure of electrical power systems is considered the primary cause of CubeSat failures within 90 days after ejection (Langer et al. 2016). For the design of a CubeSat electrical power system it is essential to calculate the

Table 3
Length of ODIN avionics bus components

Component	Length (mm)
BUS-2:	
Battery	25
EPS Board	20
On-Board Computer	15
Interface Board	25
Total	85
BUS-1:	
UHF Transceiver + GPS Board	22
S-band Transmitter	20
Magnetorquer Board	23
Total	65

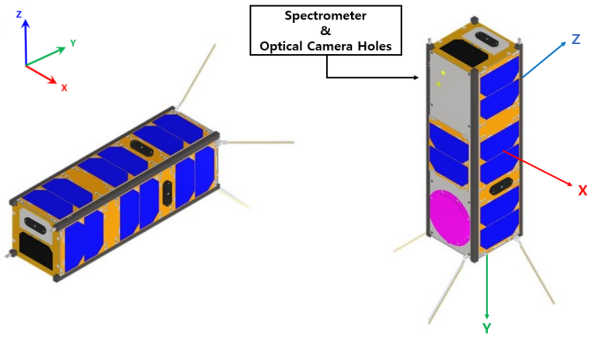

Figure 1. Overall design of ODIN.

amount of power generated during each orbit and the total power consumption during the mission. Furthermore, since the design of ODIN depends on solar panels (deployed or non-deployed) that cover the surface of the satellite body, we have calculated power generation and consumption for both varieties to identify the optimal design for ODIN.

The list of compartments used in our models is presented in Table 2.

2. CONCEPTUAL STRUCTURAL DESIGN OF ODIN

The structural design of ODIN is presented in Figure 1 which shows the non-deployed solar panel model based on the simulation result described in next section. We have set the x direction as the direction of expected satellite motion, the z direction as the radial direction (pointing away from the center of the Earth), and the y direction as the cross product between the x and z unit vectors. In this model, we have installed a total of nine solar panels on three surfaces around the satellite body. On the remaining surface, the payloads (optical camera and spectrometer) and the S-band patch antenna used for communication are placed. Another solar panel is installed onto the payload surface. Each solar panel consists of two solar cells. The efficiency and the power generating capability of solar cells are specified in the data sheet provided by Innovative Solutions In Space (ISIS).

The configuration and distribution of the bus sys-

Table 4
Mass budget of ODIN

Subsystem	Item	Mass (g)	Ratio
CDHS	DSW/OBC	100	3.19
ADCS	SOLARMEMS TECH/nanoSSOC-D60 x 3	60	1.91
	NovAtel / GPS(OEM719)	31	0.99
	CubeSpace/CubeWheel(s) x 3	180	5.74
	DSW / Magnetorquer board	225	7.18
Interface	DSW/ Interface board	100	3.19
EPS	GOMSpace / nanopower p60 (board)	80	2.55
	GOMSpace / nanopower bp4 (battery)	270	8.61
	ISIS / Solar Panel 1U x 2	100	3.19
	ISIS / Solar Panel 3U x 3	450	14.35
COMM	GOMSpace / UHF Transceiver AX100	24.5	0.78
	GOMSpace / UHF Antenna Nanocom ANT430	30	0.96
	Clydespace / CPUT S-Band CubeSat Transmitter	100	3.19
	Clydespace / CPUT S-Band Patch Antenna x2	100	3.19
STS	DSW/ 3U CubeSat Structure	800	25.51
Paylaod	X-cam / Optical Camera	85	2.71
	OceanOptics/HDX	400	12.76
Total		3135.5	78.39
Margin		864.5	21.61

Table 5
Instrument operation as function of flight mode

Part	Standby	IDLE	Science	Communication	Momentum Dumping
OBC	ON	ON	ON	ON	ON
S-band Antenna	OFF	OFF	OFF	ON	ON
S-band transmitter	OFF	OFF	OFF	ON	OFF
UHF Transceiver	Standby	Standby	Standby	ON	OFF
UHF Antenna	OFF	OFF	OFF	ON	OFF
EPS Board	ON	ON	ON	ON	ON
Battery	ON	ON	ON	ON	ON
Sun sensor	ON	ON	ON	ON	ON
Magnetometer	OFF	ON	ON	ON	ON
Gyroscope	OFF	ON	ON	ON	ON
GPS	ON	ON	ON	ON	ON
Reaction Wheel	ON	ON	ON	ON	ON
MTQ	OFF	OFF	OFF	OFF	ON
Spectrometer	OFF	OFF	ON	OFF	OFF
Camera	OFF	OFF	ON	OFF	OFF

tem of ODIN are shown in Figures 2 and 3, respectively. We placed the science payloads (miniaturized spectrometer and optical camera) together in 1U. These instruments will perform imaging and spectroscopic nadir observations of the terrestrial atmosphere. The spectrometer will provide spectroscopic information along the target direction while the optical camera will provide image data of the target region. The nadir observation mode is selected because of its simplicity in controlling the satellite. In addition, prior satellite missions conducted by NASA and ESA also adopted the nadir observation mode to retrieve the column densities of ozone and trace gases (OClO, BrO). Investigating vertical gas profiles in the terrestrial atmosphere is not in the list of the main objectives of ODIN, hence, the nadir observation is the most efficient mode for conducting scientific observation with a spectrometer. The spectrometer and optical camera will obtain light through the holes depicted in Figure 1. We placed the avionics bus in the other 2U. The lengths of the avionics bus components are presented in Table 3. As shown in Figure 4, the structural frame of ODIN limits the length of boards, thus, we divided the bus system into two parts (Bus-1 and Bus-2). The Bus-1 system consists of attitude determination/control and communication boards while the Bus-2 system consists of a power and command system board including an interface board. The interface board eases the data communication between compartment board and on board computer (OBC). Through structural modeling using computer aided design (CAD), we have verified that the designed bus model does not exceed the limits set by the frame structure.

The outer body of the satellite is covered with solar panels and communication antennas. We placed

Table 6
Power margins for the deployed solar panel design in nadir observation mode

Orbit (count)	Mode	Usage (W)	Generation (W)	Sum (W)
1	Charging	4.6	27.1	22.5
2	Observation	9.1	0	−9.1
3	Charging	4.6	27.1	22.5
4	Observation	9.1	0	−9.1
5	Charging	4.6	27.1	22.5
6	Momentum Dumping	8.4	0	−8.4
7	Charging	4.6	27.1	22.5
8	COMM	13.7	0	−13.7
9	Charging	4.6	27.1	22.5
10	Observation	9.1	0	−9.1
11	Charging	4.6	27.1	22.5
12	Observation	9.1	0	−9.1
13	Charging	4.6	27.1	22.5
14	COMM	13.7	0	−13.7
Total		104.4	189.7	85.3

Table 7
Power margins for the non-deployed solar panel design in nadir observation mode

Orbit (count)	Mode	Usage (W)	Generation (W)	Sum (W)
1	Charging	4.6	10.9	6.3
2	Observation	9.1	10.9	1.8
3	Charging	4.6	10.9	6.3
4	Observation	9.1	10.9	1.8
5	Charging	4.6	10.9	6.3
6	Momentum Dumping	8.4	10.9	2.5
7	Charging	4.6	10.9	6.3
8	COMM	13.7	10.9	−2.8
9	Charging	4.6	10.9	6.3
10	Observation	9.1	10.9	1.8
11	Charging	4.6	10.9	6.3
12	Observation	9.1	10.9	1.8
13	Charging	4.6	10.9	6.3
14	COMM	13.7	10.9	−2.8
Total		104.4	152.6	48.2

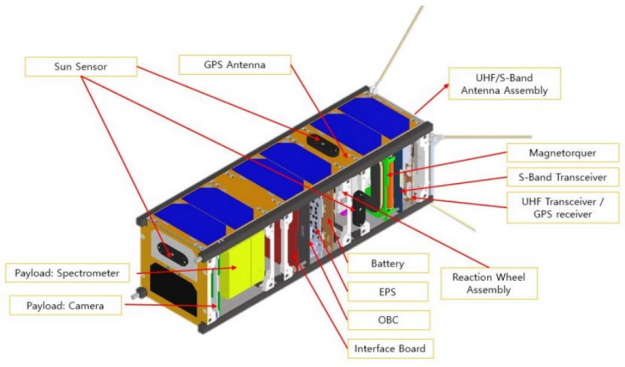

Figure 2. Configuration of ODIN.

two different antennas, one UHF antenna for uplink and one S-band patch antenna for downlink, onto the satellite body. Since S-band communication requires accurate pointing to the ground station, we have placed the S-band patch antenna on the surface of the satellite where the payload holes are located ($-z$ direction in the satellite coordinate system). The sun sensor planned to be used in determining the attitude of the satellite will also be located on the surface of the body. To determine the attitude accurately, we have placed a total of three sun sensors along the $+x$, $-y$, and $+z$ directions of the internal satellite coordinate system, respectively, with one sensor for each axis.

The mass budget of ODIN is presented in Table 4. The maximum mass allowed for a 3U CubeSat is 4 kg. The mass of each instrument is acquired from the data sheet provided by the corresponding manufacturer. As shown in Table 4, we have verified that our model does not exceed the mass limit of a 3U CubeSat. However, since the current mass budget is based on a CAD model, further investigation and measurements of the masses of individual compartments and the combined structure are required in a future study.

3. POWER GENERATION SIMULATION

We used the 'Sinda/Fluint & Thermal Desktop' software package, which is a widely used for thermal and power

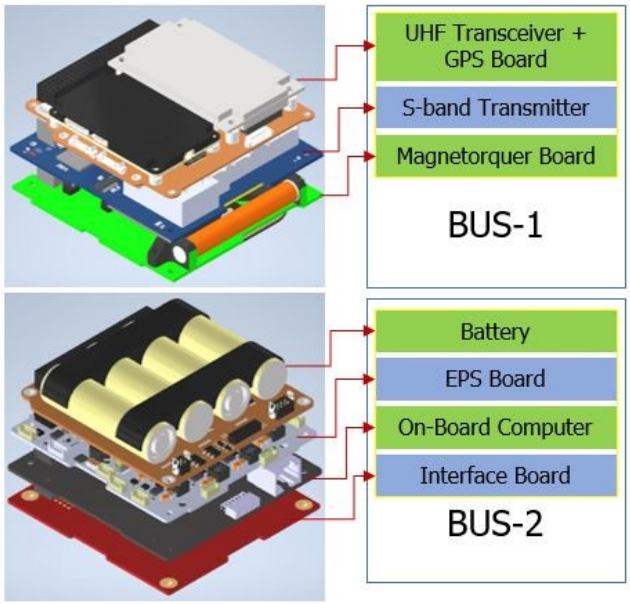

Figure 3. Avionics bus system of ODIN.

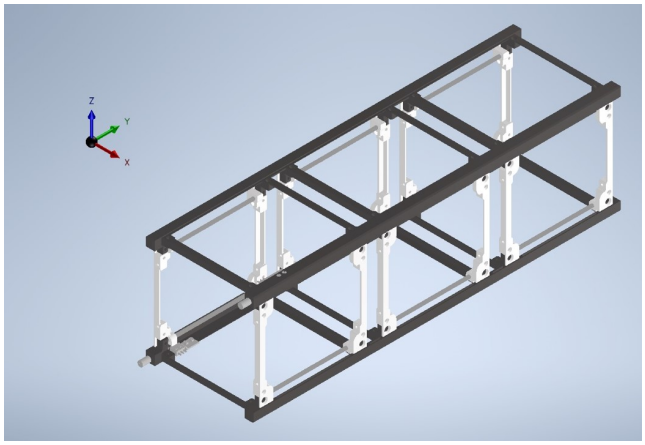

Figure 4. Structural frame of ODIN.

generation simulations of CubeSats and satellites, to analyze the power generation of ODIN in the planned orbit. Through the software, it is possible to calculate the estimated value of thermal variations of CubeSats and to estimate the power generated in given mission orbits. For selecting a configuration of solar panels it is important to estimate how much power can be generated through a mission orbit. In this study, we have calculated the power generation of two different solar panel configurations (presented in Figures 5 and 6) in two different flight modes (nadir observation mode and sun pointing mode) in the planned orbit of ODIN. The solar panels and battery used in this simulation are listed in Table 4. The power generation efficiency of the solar panels is 30%.

ODIN is supposed to be placed in the sun synchronous orbit (altitude 700 km, inclination 97°). This orbit is designated by KARI, the host of the 2019 CubeSat competition. Since ODIN will not be equipped with propulsion systems, we used the information for the

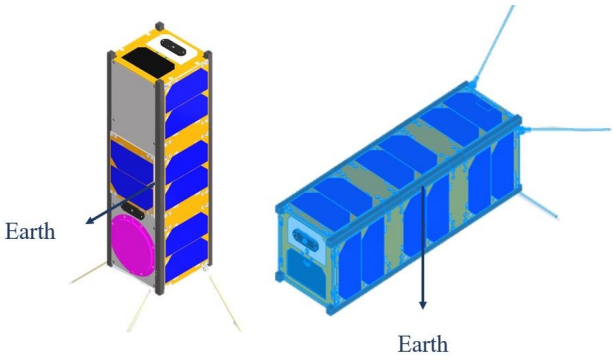

Figure 5. Non-deployed solar panel model of ODIN.

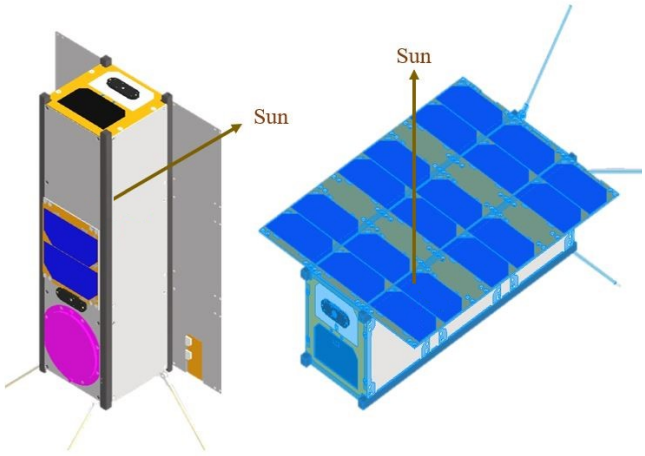

Figure 6. Deployed solar panel model of ODIN.

SSO at the estimated launch date (October 2021) to calculate the amount of generated power. The simulated orbital period is 5,926 seconds, corresponding to roughly 14 orbit cycles per day. We have specified four distinctive flight modes for ODIN: a science mode, a communication mode, an idle mode (charging mode), and a momentum dumping mode. In science mode, ODIN acquires scientific data. ODIN turns on the spectrometer and optical camera when passing the targeted latitude (latitudes ranges of 60°–80° around both poles). In communication mode, ODIN is in contact with the ground station. Its duration is restricted by the flight time of the satellite within the region of possible communication. The expected duration of passage through this region is 600 seconds. The satellite manipulates its attitude to point its antenna (S-band patch antenna) towards the ground station which is planned to be installed at Chungnam National University. During the idle mode, the satellite points its solar panels towards the sun to generate the maximum amount of power achievable in the corresponding orbit cycle. The momentum dumping mode is to release the stress on the reaction wheel. An overview of instruments operational in the various modes is provided in Table 5. We used the idle mode and the nadir observation mode to calculate the power

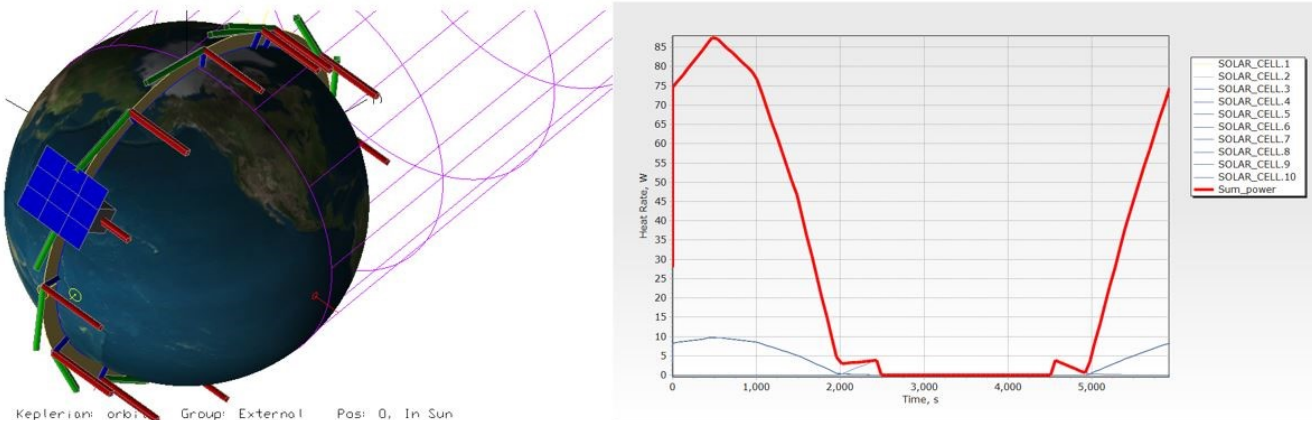

Figure 7. Simulation of power generation in nadir observation mode for the deployed solar panel model.

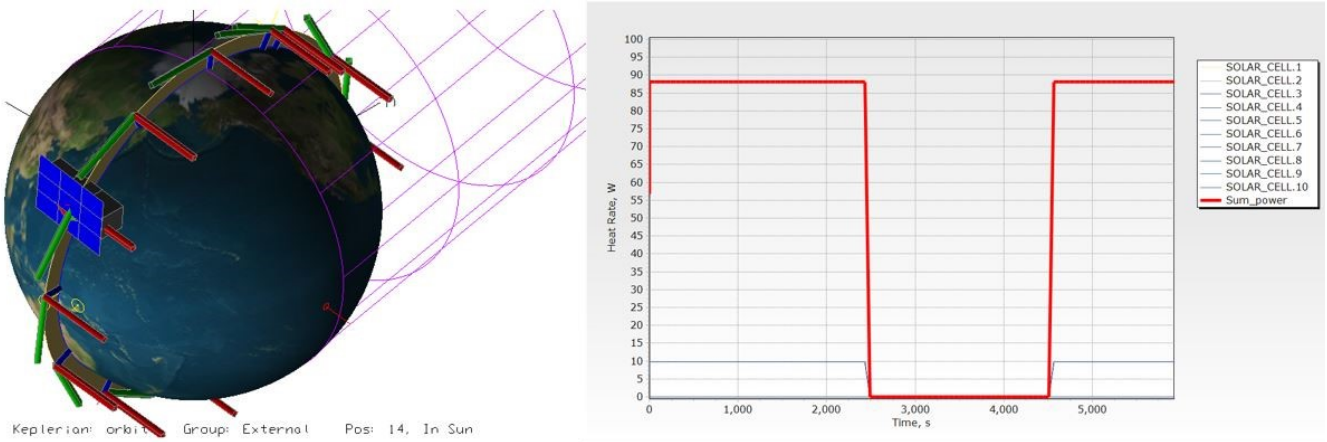

Figure 8. Simulation of power generation in Sun pointing mode (charging mode) for the deployed solar panel model.

generation. Since the fundamental purpose of this study is to find an optimized configuration of solar panels, the results for the simple attitude control mode (nadir observation mode) and the maximum power generating mode (charging mode) are selected as reference.

In the charging mode, we manipulated the solar panels of the satellite to point at the sun during a whole orbit. In the deployed solar panel design model, a total of nine solar panels points at the sun; in the non-deployed solar panel design model, three solar panels point at the sun. In the nadir observation mode, we manipulated the payloads of both models to point at the center of the Earth. The duration of charging in both nadir observation mode and charging mode (day side of the orbit) is identical at 3,780 seconds.

4. RESULTS

Simulation results for the nadir observation and the charging mode using the deployed solar panel design model are presented in Figures 7 and 8. Simulation results using the non-deployed solar panel design model are presented in Figures 9 and 10. We have verified that the deployed solar panel model yields more power than the non-deployed solar panel model in every mode. In sun pointing mode, the deployed solar panel model generated 27.1 W per orbit while the non-deployed solar panel model generated 15.2 W per orbit.

In the nadir observation mode, the deployed solar panel model generated a smaller amount of power than the non-deployed solar panel model. This is because of the pointing direction of the solar panel throughout the orbit. In case of the deployed solar panel model, the generation of power is highest when the panels point to the Sun. However, since the deployed solar panel model does not include solar panels on the surfaces of the satellite body, the power generation decreases dramatically when the pointing direction of the panels start to deviate from the direction toward the sun (see Figure 7). In case of the non-deployed solar panel model, the power generation rates remained stable because of the location of solar panels on the surfaces around the satellite body. Overall, the deployed solar panel model generated 11.6 W per orbit in average while the non-deployed solar panel model generated 10.9 W.

The power consumption requirements for ODIN are shown in Figure 11. We investigated the expected power consumption and generation of two different design models through 14 orbit cycles. For the power generation

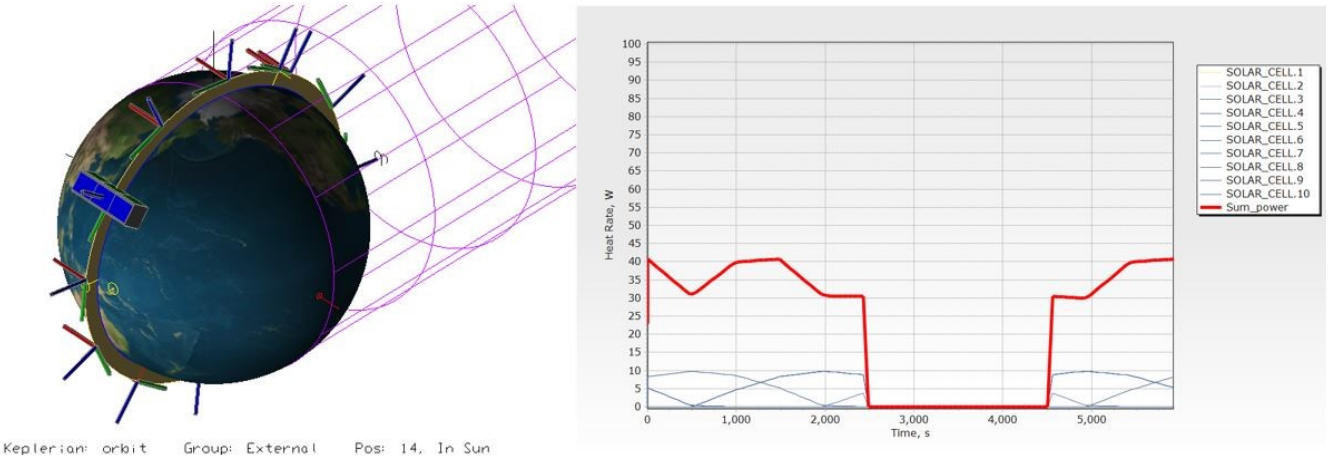

Figure 9. Simulation of power generation in nadir observation mode for the non-deployed solar panel model.

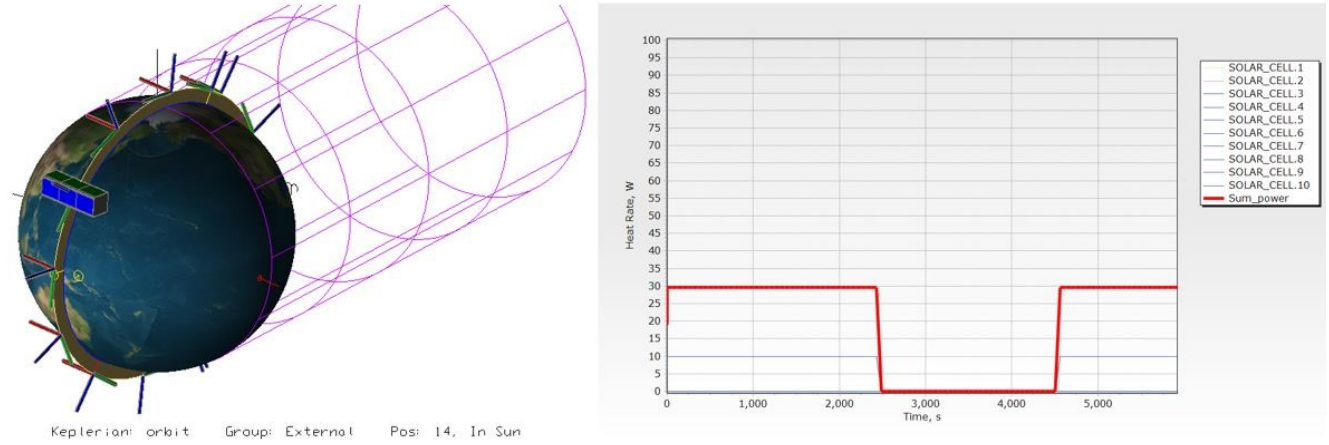

Figure 10. Simulation of power generation in Sun pointing mode (charging mode) for the non-deployed solar panel model.

in the deployed solar panel model we assumed that the solar panels of ODIN point straight at the sun through the assistance of attitude determination and the control system during the charging mode. Also, we have excluded the power generation from other orbit cycles to assess a possible worst case scenario. The power generation of the deployed solar panel model in nadir observation mode is presented in Table 6. In case of the non-deployed solar panel model in nadir observation mode, we assumed that the attitude of the satellite is remains fixed through a whole orbit. The result is presented in Table 7.

5. Discussion

We explored the conceptual structural design and estimated power generation of the ODIN CubeSat. It is crucial to design a model that complies with the general CubeSat requirements such as typical mass limit (4 kg) and constraints on structural frame designs. We have verified that the model we designed complies with the structural requirements of a 3U CubeSat. The total mass of ODIN does not exceed 4 kg and the compartments that are planned to be on board the satellite do not interfere with the structural frame of ODIN. However, since our design is based on a CAD model, detailed investigations and measurements of individual and combined models should be explored in a future study.

Utilizing the Sinda/Fluint Thermal Desktop software, we simulated the expected power generation and consumption of ODIN in SSO. We found that the deployed solar panel model generates more power than the non-deployed solar panel model in idle mode (charging mode). However, considering a full orbit cycle, we concluded that the non-deployed solar panel model is more stable in generating power due to its capability of generating power in science mode, momentum dumping mode, and communication mode whereas deployed solar panels are not able to generate power during these modes. We eventually selected the non-deployed solar panel model considering its stability against vibrations during the launch sequence as well as its capability of power generation throughout a full orbit.

Acknowledgments

We thank the undergraduate students of the ODIN CubeSat team in the Department of Astronomy and Space Science of Chungnam National University (Ms.

Sub system	Parts	Maximum Power (mW)	Stanby power	Science Mode		Communication Mode		Momentum Dumping		Idle Mode	
				Duty (%)	Energy (mWh)	Duty (%)	Energy (mWh)	Duty (%)	Energy (mWh)	Duty (%)	Energy (mWh)
C&DH	OBC	2,450	-	100%	4,091.5	100%	4,091.5	100%	4,091.5	100%	4,091.5
COMM	S-band Transmitter	5,000	300	Standby	495	100%	8,350	Standby	495	Standby	495
	UHF Transceiver	2,640	0.0825	Standby	0.136	100%	4,409	Standby	0.136	Standby	0.136
EPS	EPS Board	200	200	100%	334	100%	334	100%	334	100%	334
	Battery	100	100	100%	167	100%	167	100%	167	100%	167
ADCS	Sun Sensor (3ea)	150	50	100%	250.5	100%	250.5	100%	250.5	100%	250.5
	Magnetometer	0.33	-	100%	0.56	100%	0.56	100%	0.56	100%	0.56
	Gyroscope	12.5	-	100%	20.635	100%	20.635	100%	20.635	100%	20.635
	GPS	1,000	-	100%	1,670	100%	1,670	100%	1,670	100%	1,670
	Reaction Wheel (3ea)	2,160	360	100%	3,607.2	100%	3,607.2	100%	3,607.2	20%	721.4
	MTQ	2,000	470	0%	0	0%	0	100%	3,340	0%	0
PLS	Spectrometer	12,500		20%	4,175	0%	0	0%	0	0%	0
	Camera	1,200		20%	400.8	0%	0	0%	0	0%	0
		Available		40,000 mWh (Battery)							
		Total Usage		15,212.33mWh		22,900.40mWh		13,976.53mWh		7,750.73mWh	

Figure 11. Power budget table of ODIN.

Jeonghoon Jeong, Ms. Hyeonmin Lee, Mr. Sunho Hue, Ms. Soeun Lee, Mr. Junho Song, Mr. Kyeongsu Kim, Ms. Sohyun An, Ms. Youkyung Kim, Mr. Dongyun Kwak) for their excellent technical assistance. This work was supported by a Research Scholarship of Chungnam National University.

REFERENCES

Desselle, R., Kintziger, C., Rochus, P., et al. 2017, A 3U CubeSat to Collect UV Photometry of Bright Massive Stars, J. Small Satellites, 6, 3

Farman, J. C., Gardiner, B. G., & Shanklin, J. D. 1985, Large Losses of Total Ozone in Antarctica Reveal Seasonal ClOx/NOx Interaction, Nature, 315, 207

Han, S., Choi, Y., Cho, D., et al. 2017, Analysis of CubeSat Development Status in Korea, JKSAS, 45, 11

Iuzzolino, M., Accardo, D., Rufino G., et al. 2017, A Cubesat Payload for Exoplanet Detection, Sensors, 17, 493

Langer, M. & Bouwmeester, J. 2016, Reliability of CubeSats – Statistical Data, Developers' Beliefs and the Way Forward, 30th Annu. AIAA/USU Conf. Small Satellites

Lee, J., Park, S., Kim, Y., et al. 2017, Mission Orbit Design of CubeSat Impactor Measuring Lunar Local Magnetic Field, JASS, 34, 127

Manney, G., Santee, M., Rex, M., et al. 2011 Unprecedented Arctic Ozone Loss in 2011, Nature, 478, 469

Rigby, M., Park, S., Saito, T., et al. 2019, Increase in CFC-11 Emissions from Eastern China Based on Atmospheric Observations, Nature, 569, 546

Song, Y., Lee, D., Kim, Y., et al. 2019, Analysis on Delta-Vs to Maintain Extremely Low Altitude on the Moon and Its Application to CubeSat Mission, JASS, 36, 213

Villela, T., Costa, C., Brandao, A., et al. 2019, Towards the Thousandth CubeSat: A Statistical Overview, Int. J. Aerospace Engin.

Weatherhead, E. & Andersen S. 2006, The Search for Signs of Recovery of the Ozone Layer, Nature, 441, 39